Water Air Soil Pollut (2021) 232: 152
https://doi.org/10.1007/s11270-021-05114-2

Sorption Behavior of Dicloxacillin in Zeolites Modified with a Cationic Surfactant at Different pH

S. Alvarez-García · J. J. Ramírez-García

Received: 25 December 2020 / Accepted: 5 April 2021 / Published online: 12 April 2021

Abstract In the present work, a natural zeolite was first treated with a sodium chloride salt and subsequently modified with different cetyltrimethylammonium bromide (CTAB) concentrations for dicloxacillin removal. All the employed materials are characterized by several analytical techniques. Antibiotic sorption behavior was evaluated according to diverse parameters such as the effect of contact time, initial concentration, and pH by a batch system. Experimental results showed that the cationic surfactant treatment benefited dicloxacillin sorption. Kinetic results indicated that the equilibrium time was reached at 54 h and a maximum adsorption capacity of 1.072 and 1.051 mg/g for both modified zeolites at 25 mmol/L and 50 mmol/L, respectively. According to the kinetic data, the pseudo-second-order model adjust the best. Obtained adsorption equilibrium results, adsorption isotherms adjust well to the linear model for both adsorbents with both materials, indicating a partition mechanism. Dicloxacillin species present at different pH values and the net surface charge of the modified adsorbents influence the adsorption process.

S. Alvarez-García · J. J. Ramírez-García (✉)
Facultad de Química UAEM, Laboratorio de Análisis Instrumental, Universidad Autónoma del Estado de México, Paseo Colón esquina Paseo Tollocan S/N, Colonia, Residencial Colón, Toluca, Estado de México C.P. 50120, México
e-mail: jjramirezg@uaemex.mx

S. Alvarez-García
e-mail: sonialgar26@hotmail.com

Keywords Dicloxacillin · Cetyltrimethylammonium bromide · Zeolite · Adsorption

1 Introduction

The high population growth, the rapid development in technology, and the necessity to create numerous industries to beneficiate the society have caused an increment in contamination (Salgado-Gómez et al., 2014). In this context, water pollution by antibiotics has been considered a radical problem (Bu et al., 2013) due to their indiscriminate use and continuous incorporation into the environment by diverse sources (Behera et al., 2011; Klein et al., 2018; Weng et al., 2018). Furthermore, the presence of antibiotics in diverse water bodies negatively impacts the microbial community (Grenni et al., 2018) and have adverse effects on human health such as bacterial resistance ((WHO), 2015; Bailón-Pérez et al., 2008; Carlet et al., 2015; Cizmas et al., 2015; W. C. Li, 2014; Wu et al., 2009) and the formation of super bacteria (Anthony et al., 2018). At the same time, they can mix with other pharmaceutically active compounds (Vasquez et al., 2014), causing the possible bioaccumulation and pseudo-persistence (Kemper, 2008).

In this research line, the dicloxacillin (DCX) is a beta-lactam antibiotic widely used in humans and veterinary medicine against Gram-positive bacterial infections (Ghauch et al., 2009). Its molecular formula is $C_{19}H_{16}Cl_2N_3NaO_5S$, its weight is 510.32 g/mol, and the dissociation constants (pK_a) are of 2.8 and 10.09

(S. J. Khan & Ongerth, 2004). It is highly soluble in water (3.63 mg/L at 20 °C), and in octanol/water partition, its coefficient (*log* K_{ow}) is 2.91 (Hansch et al., 1996). A certain percentage (65 %) of this pharmaceutical product can be excreted without being metabolized through urine (Hirsch et al., 1999; S. J. Khan & Ongerth, 2004; Rivera-Gutiérrez et al., 2020), and impacting negatively in aquatic systems (Kong et al., 2016; Kümmerer, 2009; Rakić et al., 2013). Its maximum permissible limit (MPL) in water has not been reported yet, and its maximum residue limit (MRL) has been established only in European Union of 300 μg/kg (milk, muscle, and kidney fat) and 30 μg/kg (liver) (Pang, 2018).

Conventional methods have not demonstrated effective for dicloxacillin removal (Mirzaei et al., 2018), and then new alternatives such as biological degradation (Copete-Pertuz et al., 2018; Rivera-Gutiérrez et al., 2020) and oxidation advanced processes (Colina-Márquez & Castilla-Caballero, 2013; Rodriguez-Narvaez et al., 2017; Villegas-Guzman et al., 2015) have been applied. However, adsorption has been considered as a low cost, accessible, and simple process in water decontamination with different solid adsorbent materials such as granular activated carbon, clays, and zeolites (Crisafully et al., 2008; Misaelides, 2011); it has not reported yet for this antibiotic.

In this context, natural zeolites are low-cost volcanic porous minerals that have a three-dimensional structure containing AlO_4 and SiO_4 tetrahedra (Ates, 2018). Clinoptilolite zeolite is the most abundant, and its chemical formula is $(Na, K, Ca)_4Al_6Si_{30}O_{72}{*}24H_2O$ (Sprynskyy et al., 2010). According to its negative charge and hydrophilic surface, only allows inorganic pollutant removal (Misaelides, 2011). Therefore, chemical treatments with inorganic salts (Alshameri et al., 2014) or cationic surfactants (Reeve & Fallowfield, 2018) have been applied, causing the organic as well as anionic pollutant adsorption be possible (de Gennaro et al., 2014; Roxana Elena Apreutesei & Carmen Teodosiu, 2008; Rožić & Miljanić, 2011).

Even though the zeolite application for removing diverse pollutants in water is a well-studied field, it is worth mentioning specifically that CTAB-modified zeolitic materials for DCX removal have not been reported yet. Therefore, the objective of this paper was to present for the first time the dicloxacillin adsorption behavior onto a natural zeolite previously modified with cetyltrimethylammonium bromide.

2 Materials and Methods

2.1 Reagents

DCX standard (90.4% purity) was from Fersinsa; a stock solution of the antibiotic (100 mg/L) was prepared and kept at 4 °C. Cationic surfactant cetyltrimethylammonium bromide (CTAB) was from Sigma Aldrich. Acetonitrile was HPLC grade; other chemical compounds such as sodium chloride (NaCl), silver nitrate ($AgNO_3$), sodium hydroxide (NaOH), and formic acid were analytical-reagent grade. All the water employed was deionized.

2.2 Material Preparation

2.2.1 Natural Zeolite

In this work, the used natural zeolite had been collected from a San Luis Potosí, México, deposit. It is crushed in an agate mortar and sieved down to a particle size between 0.420 and 0.841 mm and identified as NZ.

2.2.2 NZ Material Treated with NaCl Salt

The natural adsorbent was firstly conditioned with a 0.1 mol/L NaCl solution by a refluxing process for 6 h. After this chemical treatment, the solids were separated by filtration and washed with deionized water until no presence of chloride ions (white precipitate) by Mohr method. Finally, the sample was labeled as NaZ.

2.2.3 NaZ Material Modified with the Cationic Surfactant

According to literature specialized, two CTAB solutions were prepared at 25 mmol/L and 50 mmol/L; both concentrations were higher than the critical micellar concentration (CMC) of CTAB surfactant (0.9 mmol/L) (Z. Li et al., 2008). The NaZ zeolite (100 g) was kept in contact with cetyltrimethylammonium bromide (25 mmol/L) in a batch system for 48 h at 30 °C under constant stirring at 100 rpm. Once the contact time is finished, the supernatant was separated by decanting, and the solids were then washed with deionized water to eliminate the surfactant excess. The modified zeolite was air-dried and identified as HZ-25. The same procedure was performed with 50 mmol/L CTAB solution, and it was then identified as HZ-50.

2.3 Adsorbent Characterization

All the zeolites in the study were characterized by diverse analytical techniques such as X-ray Powder Diffraction (XRD), Scanning Electron Microscopy (SEM) with Energy-Dispersive X-ray Spectroscopy (EDS), Fourier Transform Infrared Spectroscopy (FTIR), Thermogravimetric Analysis (TGA), BET-specific surface area (Brunauer-Emmett-Teller) analysis, and the determination of zero point charge (pH_{ZPC}).

2.3.1 X-ray Powder Diffraction

The X-ray analyzes were obtained with a SIEMMENS D5000 diffractometer (Dresden, Germany) coupled to a copper anode $\lambda = 1.5418$ Å, radiation at 40 kV with an angular sweep interval, and a rate of 5–70° and 0.03 $°s^{-1}$ in the 2θ region, respectively. The diffractograms are compared with the diffraction patterns of the Joint Committee on Powder Diffraction Standards (JCPDS).

2.3.2 Scanning Electron Microscopy with Energy-Dispersive X-ray Spectroscopy

The dried zeolites were characterized for their morphology using a scanning electron microscope JEOL model JSM 6510 (Tokyo, Japan), a low vacuum, operating at an acceleration voltage of 20 kV, work distance of 11 mm, and ×5000 of amplification by a backscattered electron detector. All the materials were previously mounted with a carbon tape and coated with gold for 2 min using a Denton Vacuum Desk IV platter (Moorestown NJ, USA) to avoid charging effects. EDS analyses were performed by energy-dispersive spectroscopy Oxford PentaFetx5 (Oxford, England).

2.3.3 Fourier Transform Infrared Spectroscopy

Analyses by FTIR were performed in the mid-infrared region (wavenumber interval of 4000 to 400 cm^{-1}) by using a Nicolet 360 FT-IR ESP (Champaign IL, USA) spectrometer. All materials were prepared with KBr pellet and 1% of zeolite.

2.3.4 Thermogravimetric Analysis

Thermal analysis was carried out using an SDT Q600 TA Instruments (New Castle DE, USA); all the samples were heated up to 950 °C, with the following operating conditions: a heating rate of 10 °C/min under N_2 atmosphere.

2.3.5 BET-Specific Surface Area (Brunauer-Emmett-Teller) Analysis

Surface area determination was performed using the Brunauer-Emmett-Teller (BET) method, through nitrogen adsorption isotherms with Autosorb IQ (Boynton Beach FL, USA) equipment at 77 K. Samples were previously heated at 100 °C for 24 h before surface areas were measured.

2.3.6 Zero Point Charge

The pH_{ZPC} experiments were carried out with 0.1 g of each zeolite and 10 mL of 0.1 M $NaNO_3$ solution at 25 °C and 100 rpm for 24 h. In this context, the initial pH (pH_o) was previously adjusted from 1.0 to 11 using a potentiometer PHM210 (Assago, Italy), with 0.1 M HCl or NaOH solutions. After the contact time, the final pH (pH) was then measured in the remaining liquid too. Each experiment was done in triplicate.

2.4 Analytical Method for DCX Determination

DCX concentration was measured by High-Performance Liquid Chromatography (HPLC). All measurements were performed using HPLC WATERS equipment with a dual UV detector 2487 model (Arcade NY, USA), an isocratic flow pump 1515 model (Arcade NY, USA), and chromatographic conditions are shown in Table 1.

The analytical method for the DCX quantification by HPLC was validated; among the evaluated parameters were detection limit (DL), quantification limit (QL), system and method linearity, suitability, system and method precision, repeatability, and accuracy according to criteria established in the International Conference on Harmonization (ICH) Guides (ICHQ2A 2009; ICHQA2B 2009).

2.5 Adsorption Experiments

2.5.1 Effect of Contact Time

The unmodified (NZ) and CTAB-modified zeolites (HZ-25 and HZ-50) were tested for DXC adsorption by batch equilibrium technique at 25 °C and 100 rpm

Table 1 Chromatographic conditions established to determinate dicloxacillin by HPLC

Column	Novapak Phenyl C18 5 μm (3.9 × 150 mm)
Wavelength (nm)	225
Mobile phase	Acetonitrile (eluent A) and formic acid 0.1% (eluent B) (60:40) (*v/v*)
Flow rate (mL/min)	0.5
Injection volume (μL)	20

in a temperature-controlled bathroom, by dispersing 0.1 g of each material by separate in 10 mL of 10 mg/L DCX solution for different time periods (0.25, 0.5, 0.75, 1, 3, 6, 9, 12, 15, 18, 21, 24, 28, 32, 36, 40, 44, 48, 54, 60, 66, and 72 h). Once the equilibrium conditions have been reached, the samples were decanted and filtered by using Millipore membranes with 0.45 μm of pore size. The supernatants were analyzed by HPLC to verify the concentration of the antibiotic released in the solution. All the tests were done in duplicate using two separate vials and the average value reported. For reference, a stock solution without zeolite was prepared and treated under the same conditions in parallel for each time contact. The amount of antibiotic adsorbed on zeolitic adsorbents at any time (q_t) in mg/g was calculated by Eq. (1):

$$q_t = \frac{(Co - Ce)V}{m} \tag{1}$$

where q_t is DCX amount per gram of zeolite (mg/g), C_o and C_e (mg/L) are the concentrations of DCX at initial and equilibrium times, respectively, V is the volume of the solution (L), and m is the mass of the used zeolite (g).

Adsorption kinetics defines the equilibrium time, the adsorption rate, the efficiency process, and mainly the possible mechanism. In this context, different kinetic models have been reported in specialized literature; among them, the pseudo-first-order (Bellú et al., 2010), pseudo-second-order (Ho & McKay, 1999), and second-order (Low, 1960) models are the most widely studied. Therefore, in this research, the kinetics models abovementioned were used to describe the employed antibiotic adsorption behavior onto NZ, HZ-25, and HZ-50 materials. The relation between the experimental data and each predicted kinetic model was determined by correlation coefficients (R^2) as well as the obtained experimental data evaluated by the pseudo-first-order, pseudo-second-order, and second-order kinetic models in their non-linearized forms using Origin 8.1 computer program, such as represented by Eq. (2), Eq. (3), and Eq. (4), respectively:

$$q_t = q_e\left(1 - exp^{-K_1 t}\right) \tag{2}$$

$$q_t = \frac{K_2 q_e^2 \mathrm{t}}{1 + K_2 q_e \mathrm{t}} \tag{3}$$

$$q_t = \frac{1}{\beta}\ln(1 + (\alpha\beta \mathrm{t})) \tag{4}$$

where q_e and q_t are DCX amounts adsorbed (mg/g) at equilibrium and at time t (h), respectively; K_1 is the pseudo-first-order adsorption rate constant (1/h); K_2 is the pseudo-second-order adsorption rate constant (g/mg h), α is the Elovich adsorption rate constant (mg/g); and β is related to the extent of surface coverage (g/mg h).

2.5.2 Dicloxacillin Adsorption Isotherms

Adsorption isotherms tests at different pH values (4.0, without adjust, and 9.0) were performed only with HZ-25, and HZ-50 materials; by employing 10 mL of DCX solutions at different concentrations (0.3, 0.5, 1.0, 1.5, 3.0, 5.0, 6.0, 8.0, 9.0, 10.0, 12.0, 14.0, 16.0, 18.0 and 20.0 mg/L) with 0.1 g of each material. The initial pH of the solution was previously adjusted using 0.1 M HCl or NaOH solutions and measured with a PHM210 Standard pH Meter (Assago, Italy). All the samples were shaken for 54 h at 25 °C and 100 rpm by batch equilibrium technique. The pH was monitored and adjusted. After reaching equilibrium time, the samples were treated and analyzed using HPLC as abovementioned in Section 2.5.1. All adsorption tests were run in duplicate.

The equilibrium studies for an adsorption process can be modeled by Langmuir (Langmuir, 1917), Freundlich (Hashemian et al., 2013), and Langmuir-Freundlich (Turiel et al., 2003) isotherm models because they are the most frequently applied in specialized literature. Then, the obtained data were evaluated with adsorption isotherm models abovementioned, in their not linearized form using Origin 8.1 computer program, such as represented by Eq. (5), Eq. (6), and Eq. (7), respectively:

$$q_e = \frac{q_{\max} K_L C_e}{1 + K_L C_e} \quad (5)$$

$$q_e = K_F C_e^{1/n} \quad (6)$$

$$q_e = \frac{q_{\max} K_{LF} C_e^{1/n}}{1 + K_{LF} C_e^{1/n}} \quad (7)$$

where C_e is DCX concentration in solution at equilibrium (mg/L), q_e is DCX amount adsorbed at equilibrium (mg/g), and K_L and q_{max} are the Langmuir constants, related to the affinity between an adsorbent and adsorbate (L/mg) and the maximum adsorption capacity (mg/g), respectively. K_F is the Freundlich adsorption constant, related to the adsorption capacity of the adsorbent (L/g), *1/n* is the energy of adsorption effectiveness of zeolitic material calculated, and K_{LF} is the Langmuir-Freundlich adsorption constant related to the adsorption capacity of the adsorbent calculated (L/g).

3 Results and Discussion

3.1 Adsorbent Characterization Results

3.1.1 X-ray Diffraction

The mineral composition and crystalline structure were analyzed by XRD measurements as shown in Fig. 1, which describes that all zeolites show well-defined peak characteristics with high intensity.

Figure 1a shows the details of the NZ XRD pattern; it can be observed that the main mineral component was clinoptilolite (JCPDS 25-1349); also, other lower intensity peaks such as quartz (JCPDS 33-1161) and Halite (JCPDS 89-3615) were present too. In the NaZ diffractogram (Fig. 1b) the same components that NZ are shown; they do not differ in intensity reflection peaks, and there are no changes in their position. This result suggests that there were not any changes in the zeolite structure after the NaCl treatment. On the other hand, only in HZ-25 material, a slight shift and an intensity magnification in one peak were only observed in the interval 20–30° in 2θ degrees, in comparison with HZ-50 zeolite; this phenomenon can attribute to the CTAB effect over the NaZ external surface. Therefore, it is inferred that the clinoptilolite structure was maintained after CTAB treatment as shown in Fig. 1 c and d.

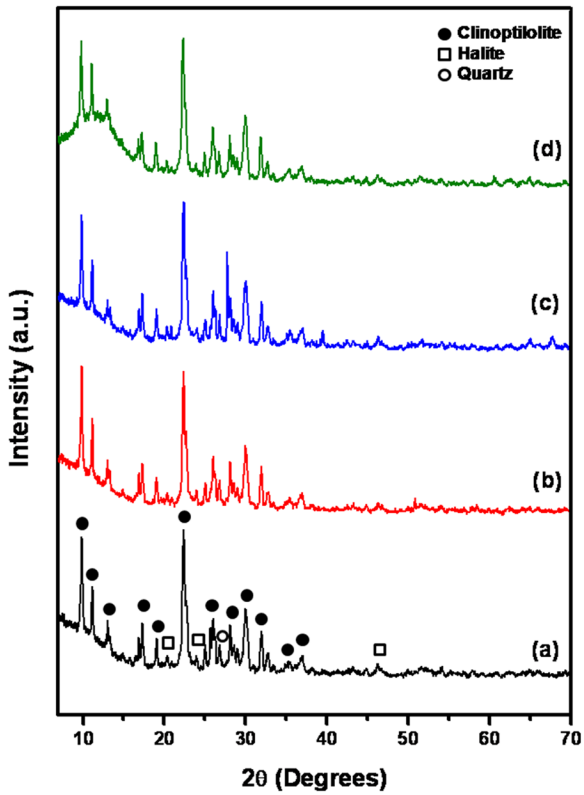

Fig. 1 X-ray diffractograms of zeolites: (**a**) NZ, (**b**) NaZ, (**c**) HZ-25, and (**d**) HZ-50

All the XDR results agreed with other author results (Dávila-Estrada et al., 2016; Torres-Pérez et al., 2007).

3.1.2 Scanning Electron Microscopy with Energy-Dispersive X-ray Spectroscopy

The morphology of the studied zeolites, performed by SEM at ×5000 magnification, is shown in Fig. 2. In all the materials, can be appreciated a rough surface with cavities, and the typical clinoptilolite crystals as euhedral plates and laths characterized by a monoclinic structure. The NZ material presents bigger and wider cubic or coffin-shaped crystals (Fig. 2a) in comparison with NaZ zeolite; the crystal size changes could be attributed to the NaCl treatment (Fig. 2b). The CTAB-modified zeolites (HZ-25 and HZ-50) maintained their morphological features after treatment; only the crystal sizes were affected (Fig. 2 c and d). However, only in the first CTAB-modified adsorbent that a slight coating was observed due to surfactant presence on the zeolite surface. The obtained SEM results were similar with previously reported (Elsheikh et al. 2017).

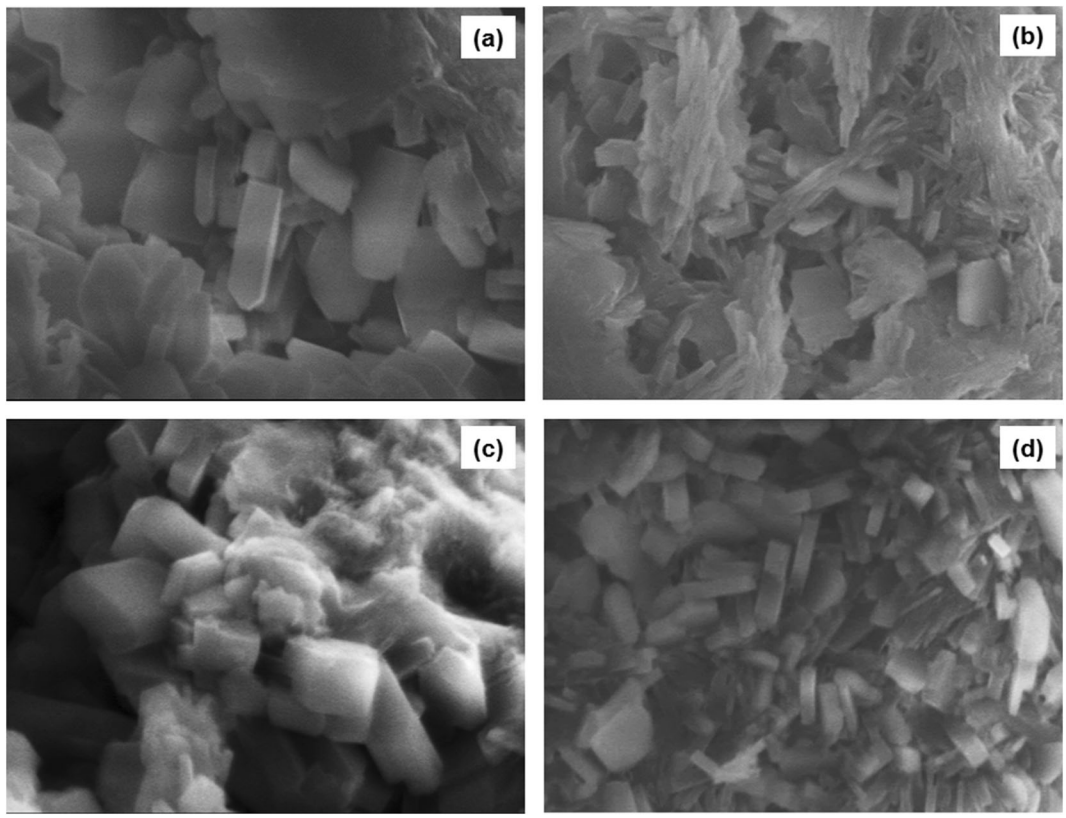

Fig. 2 Scanning electron micrograph of zeolites at ×5000 magnification: (**a**) NZ, (**b**) NaZ, (**c**) HZ-25, and (**d**) HZ-50

The chemical elemental composition of the employed materials is reported in Table 2. All the samples were constituted mainly by Si, Al, and O which form the aluminosilicates framework. Other elements such as Ca^{2+}, K^{+}, Na^{+}, Fe^{2+}, and Mg^{2+} are present in minor proportion, in order of abundance. After NZ material was treated with NaCl solution, and the amount of sodium increased; also, it can be observed that the

Table 2 Chemical composition of all the zeolites determined by EDS

Element	NZ (wt. %)	NaZ (wt. %)	HZ-25 (wt. %)	HZ-50 (wt. %)
O	61.52± 7.78	59.71 ± 9.64	62.11± 4.51	63.03± 1.73
Na	0.62 ± 0.17	1.21 ± 0.28	0.97 ± 0.16	1.08 ± 0.09
Mg	0.34 ± 0.04	0.34± 0.10	0.24 ± 0.05	0.24 ± 0.08
Al	5.90 ± 0.48	5.41± 0.84	4.04 ± 0.66	4.30 ± 0.50
Si	25.34 ± 3.35	25.20± 6.30	17.04± 3.58	17.83 ± 2.02
K	1.91± 0.79	1.53 ± 0.74	1.32 ± 0.64	0.95 ± 0.17
Ca	2.21 ± 0.98	1.70 ± 0.94	1.06 ± 0.56	0.91 ± 0.20
Fe	-----	0.44 ± 0.26	0.47 ± 0.37	0.22 ± 0.17
N	-----	-----	6.34± 2.94	4.94 ± 0.35
C	-----	-----	6.42± 1.13	6.52± 1.90
Cl	-----	-----	-----	-----
Br	-----	-----	-----	-----

amount of potassium and calcium decreased, which indicates that salt treatment allowed the Na^+ incorporation to the clinoptilolite structure, and it preferably exchanged only with these ions. This behavior could be due to their ionic radius, preference of monovalent ions, and place in the zeolite structure (Rasouli et al., 2012). Subsequently, carbon and nitrogen were only presented in both modified zeolites. On the other hand, the amount of sodium in HZ-25 and HZ-50 was lower than in NaZ material due to the amino groups of the cationic surfactant as reported (Sonia Alvarez-García et al., 2019). The Cl and Br absence confirm that the washings were performed correctly.

3.1.3 Fourier Transform Infrared Spectroscopy

Figure 3 shows the FTIR spectra of the studied adsorbents. In all the spectra appear the same signals, the bands related to internal tetrahedral vibrations of Si-O-Si or Al-O-Si bridges in the 1200–400 cm^{-1} region, two bands characteristic of clinoptilolite in 3800–3420 cm^{-1}, and the OH-stretching vibrations of the molecular water about 1640 cm^{-1}. The intensity of the band around 1000 cm^{-1} diminished after the conditioning with the inorganic salt as shown in Fig. 3b; this was previously reported by other authors (Montes-Luna et al., 2015). Finally, CTAB modification caused changes in two groups of bands: the first related to hydroxyls and molecular water and the second with the surfactant presence (Fig. 3 c and d). In this context, the band around 3640 cm^{-1} did not show any visual modification, but the position and intensity of the bands in 3500–3050 cm^{-1} regions decreased. Some researchers have mentioned that the position and intensity depend on the surfactant concentration (Mozgawa et al., 2011). On the other hand, intense bands about 2939 cm^{-1} and 2897 cm^{-1} confirmed the CTAB presence; signals in the ranges of 2924–2918 cm^{-1} and 2851–2850 cm^{-1} correspond to the asymmetric and symmetric CH_2 stretching vibration, respectively (Guan et al., 2010). As it is clearly evident, their intensity increases when CTAB increases, and both signals were shifted to lower wavenumbers; this phenomenon has been observed in other studies (Barczyk et al., 2014; Rasouli et al., 2012).

3.1.4 Thermogravimetric Analysis

Figure 4 describes degradation patterns of all the studied zeolites through temperature ranges of mass

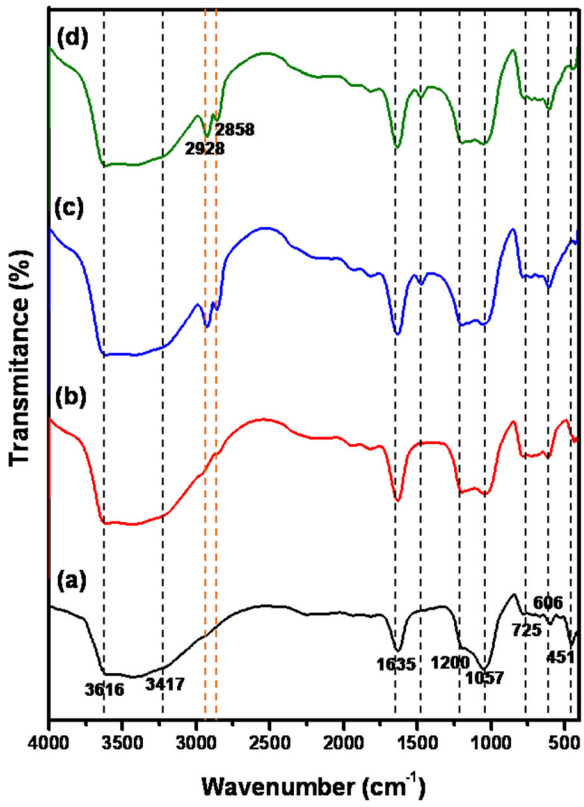

Fig. 3 FTIR spectra of zeolites: (**a**) NZ, (**b**) NaZ, (**c**) HZ-25, and (**d**) HZ-50

loss. Full weight loss was of 11.80 %, 11.06 %, 14.38 %, and 12.19 % for NZ, NaZ, HZ-25, and HZ-50 materials, respectively.

According to diverse authors, thermal decomposition of a zeolite involucres a first stage associated with a weight loss due to superficial water desorption or a dehydration process by weak bounds. Subsequently, a second stage was attributed to the crystallization water loss; in this case, the water molecules are coordinated to the interchangeable cations within the zeolite structure. And finally, a third stage associated with the release of hydroxyl groups from the clinoptilolite structure (Corral-Capulin et al., 2018). In this context, the natural zeolites contain large channels that let access to some chemical species, and their dehydration occurs below 400 °C; it , for this reason, can be mentioned that the weight loss of zeolite below this temperature does not affect the zeolite structural stability (Colella & Wise, 2014).

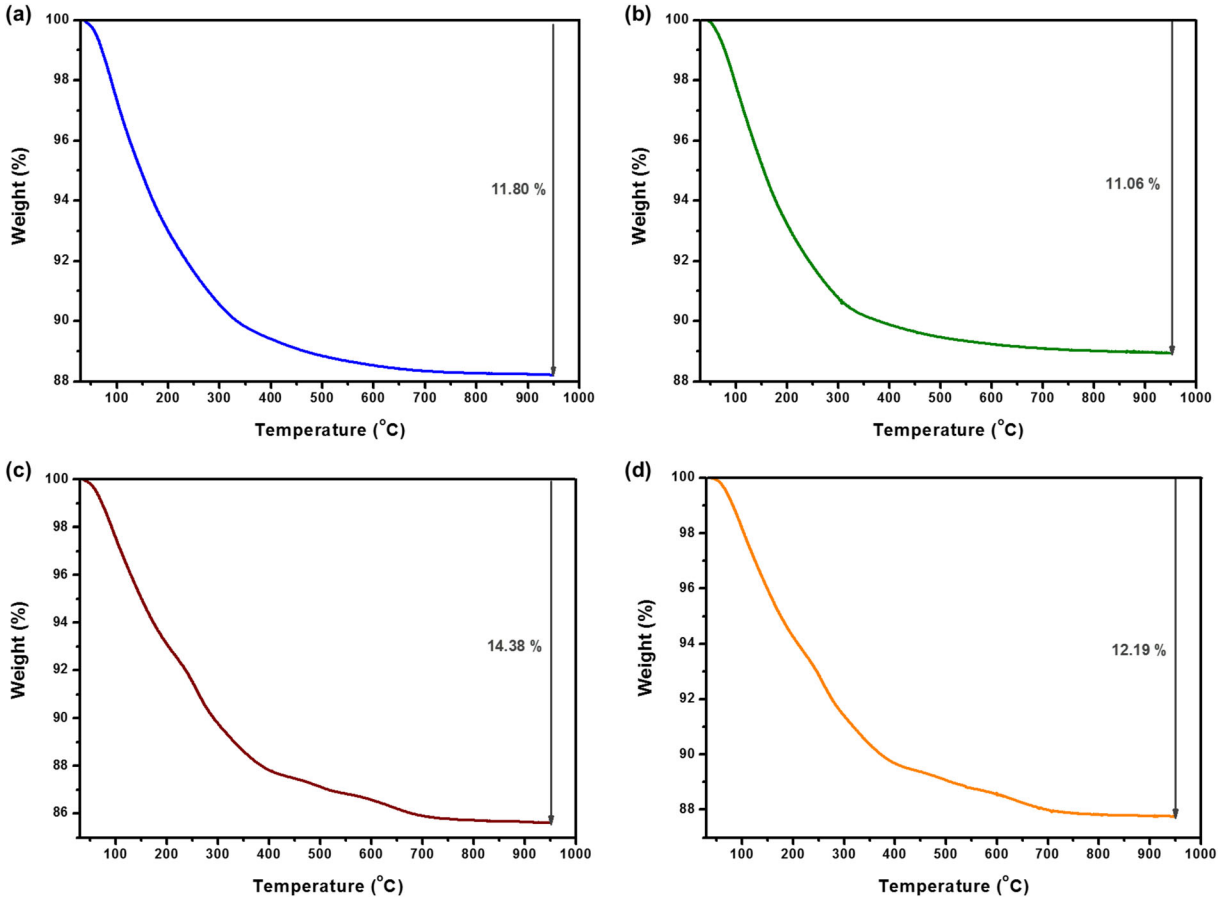

Fig. 4 Thermogravimetric curve of zeolites: (**a**) NZ, (**b**) NaZ, (**c**) HZ-25, and (**d**) HZ-50

3.1.5 BET-Specific Surface Area (Brunauer-Emmett-Teller) Analysis

The BET-specific surface areas for NZ, HZ-25, and HZ-50 are shown in Table 3. Natural zeolite has the largest surface area (28.4 m^2/g); this value agrees with the results reported by other authors (Sonia Alvarez-García et al., 2019). Regarding CTAB-modified zeolites, their areas were lower (16.1 and 10.7 m^2/g, respectively) than NZ, as a result of the surfactant dimensions blocked some main channels of the clinoptilolite as previously mentioned in several researchers (S. Alvarez-García et al., 2018; Reeve & Fallowfield, 2018).

3.1.6 Zero Point Charge

In this work, the adsorbent burden was determined to understand the interaction between DCX antibiotic and zeolite in the adsorption process; this parameter indicates the material load at different pH values. Therefore, pH_{ZPC} is the pH where the total charge of the particles of the adsorbent surface is zero (M. N. Khan & Sarwar, 2007). The experimental results for pH_{ZPC} in all the zeolites are presented in Table 4. The obtained pH_{ZPC} was 6.38, 6.21, 5.86, and 5.75 for NZ, NaZ, HZ-25, and HZ-50 materials, respectively. At pH values lower than pH_{ZPC}, the adsorbent surface is negatively charged due to deprotonation reactions of OH^- groups present in the adsorbent, pH values equal to pH_{ZPC} indicate a neutral surface charge, while at pH values

Table 3 Specific surface areas of all the zeolites determined by BET method

Zeolite	Specific surface area
NZ	28.4
HZ-25	16.1
HZ-50	10.7

Table 4 Zero point charge of all the zeolites determined by potentiometric determination

Zeolite	pH_{ZPC}
NZ	6.38
NaZ	6.21
HZ-25	5.86
HZ-50	5.75

higher than pH_{ZPC}, and the material surface has a positive charge as a result of the OH^- protonation in the zeolite structure.

3.2 Analytical Method for Dicloxacillin Determination

A solution of 100 mg/L DCX was prepared and analyzed by HPLC under the previously established chromatographic conditions. The obtained retention time was 3.59 min as shown in Fig. 5.

The analytical method for the quantification of DCX by HPLC demonstrated to be accurate, precise, and trustworthy according to acceptance criteria established in the International Conference on Harmonization (ICH) Guides as shown in Table 5.

where r^2 is the coefficient of correlation, *CV* is the coefficient of variation between each injection of the samples, *CI* is the confidence interval, *T* is the tailing factor that indicates the symmetry of the peak, and *N* is the theoretical plates of the used column.

3.3 Adsorption Experiment Results

3.3.1 Dicloxacillin Adsorption Kinetic Results

Figure 6 shows the relationship between the contact time (t) and the DCX adsorption capacity (q_t) over NZ, HZ-25, and HZ-50 materials. The results indicated that dicloxacillin can be adsorbed only onto CTAB-modified zeolites. The amount of antibiotic adsorbed rises rapidly in the first 24 h and reaches equilibrium adsorption at 54 h of contact time with a q_t value of 1.072 mg/g and 1.051 mg/g for HZ-25 and HZ-50 materials, respectively. Therefore, it can be inferred that the treatment with the cationic surfactant had a considerable impact over the q_t in comparison with NZ zeolite due to the hydrophobic character of their surface.

The kinetic parameters were evaluated by pseudo-first-order, pseudo-second-order, and second-order kinetic models by non-linear regression analysis as shown in Table 6. According to the obtained results, it can be inferred that the obtained data for the natural zeolitic material (NZ) did not fit well with any model. On the other hand, the pseudo-second-order model was the most appropriate for describing the DCX adsorption for both CTAB-modified adsorbents considering that this presented the highest correlation coefficient (R^2); the obtained q_e value was very close to experimental q_e in both materials, although the Residual Sum of Squares (*RSS*) value was not the lowest in the two CTAB-modified materials compared with the other two evaluated models. Finally, it observed that the adsorption was higher than desorption due to α and β values obtained in the second-order kinetic model.

Adsorption has been used as an alternative removal method for diverse pharmaceuticals. Unfortunately, an adsorption study with modified zeolites with CTAB has not been reported before. However, Table 7 shows the results determined by other authors using different removal methods. As can be observed in the table, the results in this work are very closed to the other methods.

3.3.2 Dicloxacillin Adsorption Isotherm Results

The pH of the adsorbate from the aqueous medium that is fundamental in a removal process due to any variation in pH influences not only on the present

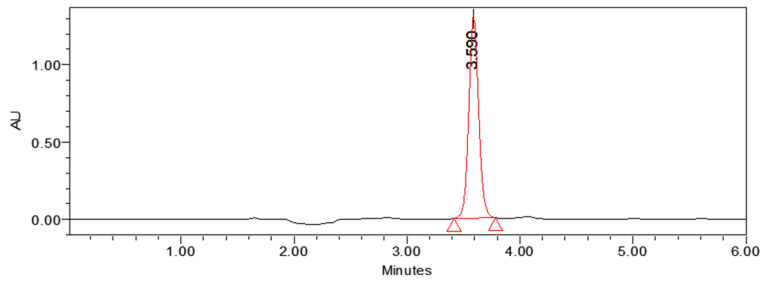

Fig. 5 Chromatogram of 100 mg/L dicloxacillin by HPLC

Table 5 Validation results of the method for the quantification of dicloxacillin by HPLC

Parameter	Experimental result	Acceptance criteria
Detection limit*	0.1 mg/L	-----
Quantification limit*	1 mg/L	-----
System linearity	$r^2 = 0.999$	$r^2 \geq 0.98$ with minimum 5 points
Method linearity	$r^2 = 0.999$ $CV = 1.24$ CI (μ) = 98.65–101.13 %	$r^2 \geq 0.98$ $CV \leq 1.50$ *CI* (μ) must include 100%
System precision	$CV = 1.18$	$CV \leq 1.50$
Suitability	$CV = 0.85$ $T = 1.47$ $K' = 2.56$ $N = 4042$	$CV \leq 2.00$ $T \leq 2.00$ $K' \geq 2.00$ $N \geq 2000$
Repeatability and accuracy	$CV = 1.90$ *CI* (μ) = 97.38–101.18 %	$CV \leq 2.00$ CI (μ) must include 100%
Method precision	$CV = 1.27$	$CV \leq 2.00$ for 2 analysts in 2 different days

*Determined by the signal-to-noise method

species but also on the net surface charge of the adsorbent (Misaelides, 2011; Reeve & Fallowfield, 2018. In this context, the performance of CTAB-modified zeolites as a function of DCX concentrations at different pH values (4.0, without adjusted of pH, and 9.0) was evaluated using the adsorption isotherms, as shown in Fig. 7. A contact time of

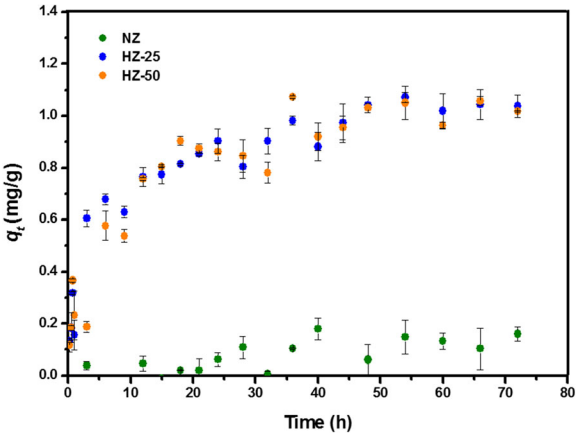

Fig. 6 Adsorption kinetics of dicloxacillin onto studied zeolitic materials

Table 6 Kinetic parameters of dicloxacillin adsorption from aqueous medium onto zeolites

Kinetic models	Parameters	Zeolites		
		NZ	HZ-25	HZ-50
Pseudo-first order	q_e (mg/g)	Do not adjusted	0.939	0.979
	K_1 (1/h)		0.203	0.116
	R^2		0.880	0.895
	RSS		0.227	0.225
Pseudo-second order	q_e (mg/g)	Do not adjusted	1.033	1.112
	K_2 (g/mg h)		0.283	0.143
	R^2		0.939	0.912
	RSS		0.116	0.189
Second order	α (mg/g)	Do not adjusted	15.999	12.024
	β (g/mg)		0.397	0.410
	R^2		0.961	0.908
	RSS		0.074	0.171
q_e exp		0.148	1.072	1.051

54 h was selected for the determination of the adsorption isotherms to ensure that equilibrium sorption has been reached. From the figure, it can be observed that the amount of DCX adsorbed increases with increasing concentration in the solution for both CTAB-modified materials. However, the adsorption behavior was different, in Fig. 7a,the highest DCX adsorption is shown at pH 9.0, the isotherm without adjusted pH shows an intermediate value, and the lower adsorption is found at pH 4.0 with HZ-25 material. On the other hand, the maximum adsorption capacity in the other modified zeolite was obtained without adjusted of pH, the intermediate value was at pH of 4.0, and the lower adsorption capacity is found for the pH of 9.0, as shown in Fig. 7b.

The DCX contains -NH and -COOH, which can be combined with the H^+ and OH^- groups in solution

Table 7 Dicloxacillin elimination with different removal methods

Removal method	% eliminated	References
Adsorption with HZ-25	95.39	This work
Adsorption with HZ-50	96.52	This work
Biodegradation	100.0	Rivera-Gutiérrez et al. (2020)
Indian almond leaf	86.93	Ghimire et al. (2019)

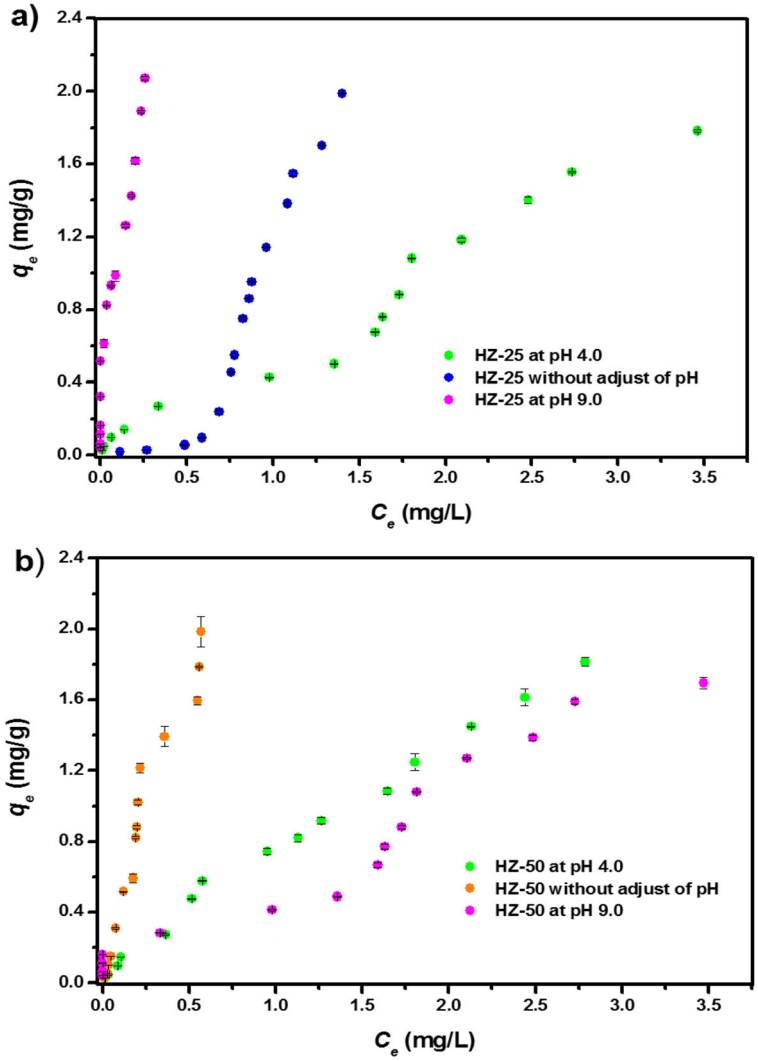

Fig. 7 Adsorption isotherms of dicloxacillin at different pH values onto (**a**) HZ-25 and (**b**) HZ-50 materials

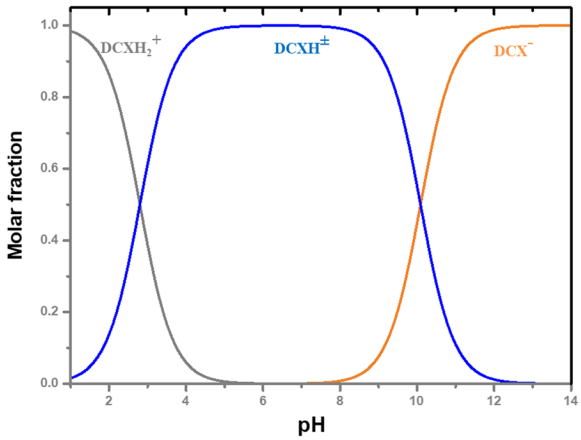

Fig. 8 Chemical species distribution of dicloxacillin

respectively so that the DCX can exist in solution in three forms including cation, zwitterion, and anion. According to its pK_a value (pK_{a1} = 2.8, pK_{a2} = 10.09), the antibiotic proportion in different forms can be calculated as shown in Fig. 8.

When pH is lower than pK_{a1}, -NH in DCX can form $DCXH^+$ by combining with H^+ in solution, which does not benefit the DCX adsorption on the negatively charged surface of HZ-25 zeolite. In the pH range of 3 to 10, most of DCX is cationic. With pH increasing, the DCX cations in the solution decrease, while neutral ions gradually increase. When pH = 5.86, the DCX almost exists in electrically neutral zwitterionic form, and the DCX cationic groups can easily adsorb on the positively charged surface of HZ-25 zeolite. On the other hand,

Table 8 Isotherm parameters for dicloxacillin adsorption onto HZ-25 and HZ-50 materials from aqueous medium

Isotherm model	Parameters	HZ-25 zeolite			HZ-50 zeolite		
		pH 4.0	Without adjusted of pH	pH 9.0	pH 4.0	Without adjusted of pH	pH 9.0
Langmuir	q_{max} (mg/g)	Do not adjusted	Do not adjusted	2.643	6.861	4.548	Do not adjusted
	K_L			8.654	0.125	0.220	
	R^2			0.881	0.993	0.957	
	RSS			0.706	0.033	0.239	
Freundlich	*n*	0.920	0.473	2.824	1.204	1.719	0.944
	1/n	1.087	2.114	0.354	0.831	0.582	1.059
	K_F	0.489	1.053	2.000	0.765	2.000	0.498
	R^2	0.965	0.940	0.664	0.995	0.834	0.944
	RSS	0.150	0.335	2.118	0.022	0.927	0.238
Langmuir-Freundlich	*n*	1.788	5.761	Do not adjusted	Do not adjusted	1.630	2.735
	1/n	0.559	0.174			0.613	0.366
	K_{LF}	0.140	1.574			8.976	0.169
	q_{max} (mg/g)	3.277	2.059			2.302	2.103
	R^2	0.964	0.991			0.964	0.952
	RSS	0.144	0.047			0.183	0.185
Linear	K_d	0.527	1.092	8.422	0.681	3.495	0.523
	R^2	0.965	0.737	0.816	0.983	0.913	0.946

with HZ-50 zeolite, the DCX adsorption behavior is different; it may be due more for the arrangement of the cationic surfactant.

In order to describe the adsorption isotherm further, the experimental results were analyzed by non-linear equations of Langmuir, Freundlich, and Langmuir-Freundlich models using Origin 8.1 computer software. However, some authors have proposed that the adsorption of organic pollutants by cationic surfactant-modified zeolitic materials could be the partition mechanism (Krajišnik et al., 2011). Therefore, the experimental results were also analyzed by the linear model.

Although Freundlich and Linear model were the only ones that presented adjustment at different pH as shown in Table 8, the linear model presented the best adjustment with the experimental data due to the visible linear form of the figures, indicating a partitioning mechanism. In addition, it can be observed that the adsorption capacity increases with increasing the initial concentration of dicloxacillin in both modified zeolites at different pH; this behavior matches with other authors (Dávila-Estrada et al., 2016). However, the value of partitioning coefficient, K_d, only increases with increasing the pH value for HZ-25 zeolite.

4 Conclusions

The present study demonstrated that a natural zeolite, such as clinoptilolite, modified with a cationic surfactant, in this case CTAB, allows the removal of dicloxacillin in aqueous solution. The kinetic model of pseudo-second-order (Ho) is the one that best describes the adsorption behavior of dicloxacillin in an aqueous medium for the modified zeolite at 25 mmol/L and 50 mmol/L of CTAB. The adsorption isotherms at different pH follow a linear behavior which indicates a partition mechanism where the dicloxacillin dissolves with the organic phase due to aliphatic chains of the cationic surfactant. The modification of natural zeolite (originally from San Luis Potosi) with the cationic surfactant improved material efficiency to dicloxacillin removal. The pH is a parameter that directly affects dicloxacillin adsorption on the zeolite modified with CTAB.

Acknowledgements The authors acknowledge the financial support from the CONACYT (Project 215997) and CONACYT scholar Grant No. 553982 for SAG.

Declarations

Conflict of Interests The authors declare no competing interests.

References

(WHO), W. H. O (2015). Global action plan on antimicrobial resistance. WHO Press, 1–28. ISBN 978 92 4 150976 3

Alshameri, A., Ibrahim, A., Assabri, A. M., Lei, X., Wang, H., & Yan, C. (2014). The investigation into the ammonium removal performance of Yemeni natural zeolite: Modification, ion exchange mechanism, and thermodynamics. *Powder Technology*. https://doi.org/10.1016/j.powtec.2014.02.063.

Alvarez-García, S., Ramírez-García, J. J., Granados-Correa, F., & Sánchez-Meza, J. C. (2018). Determination of kinetic, isotherm, and thermodynamic parameters of the methamidophos adsorption onto cationic surfactant-modified zeolitic materials. *Water, Air, & Soil Pollution, 229*(11), 347. https://doi.org/10.1007/s11270-018-3995-7.

Alvarez-García, S., Ramírez-García, J. J., Granados-Correa, F., & Sánchez-Meza, J. C. (2019). Structural and textural influences of surfactant-modified zeolitic materials over the methamidophos adsorption behavior. *Separation Science and Technology, 00*(00), 1–16. https://doi.org/10.1080/01496395.2019.1568476.

Anthony, A. A., Adekunle, C. F., & Thor, A. S. (2018). Residual antibiotics, antibiotic resistant superbugs and antibiotic resistance genes in surface water catchments: Public health impact. *Physics and Chemistry of the Earth, 105*(March 2017), 177–183. https://doi.org/10.1016/j.pce.2018.03.004.

Ates, A. (2018). The modification of aluminium content of natural zeolites with different composition. *Powder Technology*, #pagerange#. https://doi.org/10.1016/j.powtec.2018.12.018

Bailón-Pérez, M. I., García-Campaña, A. M., Cruces-Blanco, C., & del Olmo Iruela, M. (2008). Trace determination of β-lactam antibiotics in environmental aqueous samples using off-line and on-line preconcentration in capillary electrophoresis. *Journal of Chromatography A, 1185*(2), 273–280. https://doi.org/10.1016/j.chroma.2007.12.088.

Barczyk, K., Mozgawa, W., & Król, M. (2014). Studies of anions sorption on natural zeolites. *Spectrochimica Acta - Part A: Molecular and Biomolecular Spectroscopy*. https://doi.org/10.1016/j.saa.2014.06.065.

Behera, S. K., Kim, H. W., Oh, J. E., & Park, H. S. (2011). Occurrence and removal of antibiotics, hormones and several other pharmaceuticals in wastewater treatment plants of the largest industrial city of Korea. *Science of the Total Environment, 409*(20), 4351–4360. https://doi.org/10.1016/j.scitotenv.2011.07.015.

Bellú, S., Sala, L., González, J., García, S., & Frascaroli, M. (2010). Thermodynamic and dynamic of chromium biosorption by pectic and lignocellulocic biowastes. *Journal of Water Resource and Protection, 02*(10), 888–897. https://doi.org/10.4236/jwarp.2010.210106.

Bu, Q., Wang, B., Huang, J., Deng, S., & Yu, G. (2013). Pharmaceuticals and personal care products in the aquatic environment in China: A review. *Journal of Hazardous Materials, 262*, 189–211. https://doi.org/10.1016/j.jhazmat.2013.08.040.

Carlet, J., Aaron, L., Abassi, M. S., Abbo, L., Aboderin, O., Abraham, E., et al. (2015). World alliance against antibiotic resistance: The WAAAR declaration against antibiotic resistance. *Medicina Intensiva, 39*(1), 34–39. https://doi.org/10.1016/j.medin.2014.10.004.

Cizmas, L., Sharma, V. K., Gray, C. M., & McDonald, T. J. (2015). Pharmaceuticals and personal care products in waters: Occurrence, toxicity, and risk. *Environmental Chemistry Letters, 13*(4), 381–394. https://doi.org/10.1007/s10311-015-0524-4.

Colella, C., & Wise, W. S. (2014). The IZA handbook of natural zeolites: A tool of knowledge on the most important family of porous minerals. *Microporous and Mesoporous Materials*. https://doi.org/10.1016/j.micromeso.2013.08.028.

Colina-Márquez, J. Á., & Castilla-Caballero, D. R. (2013). Mineralización fotocatalítica de agua residual contaminada con dicloxacilina comercial en un reactor solar CPC a escala piloto Photocatalytic mineralization of wastewater polluted with commercial dicloxacillin in a pilot-scale solar CPC reactor. *Ingeniería y Competitividad, 15*(161–16), 161–169.

Copete-Pertuz, L. S., Plácido, J., Serna-Galvis, E. A., Torres-Palma, R. A., & Mora, A. (2018). Elimination of isoxazolyl-penicillins antibiotics in waters by the ligninolytic native Colombian strain Leptosphaerulina sp. considerations on biodegradation process and antimicrobial activity removal. *Science of the Total Environment, 630*, 1195–1204. https://doi.org/10.1016/j.scitotenv.2018.02.244.

Corral-Capulin, N. G., Vilchis-Nestor, A. R., Gutiérrez-Segura, E., & Solache-Ríos, M. (2018). The influence of chemical and thermal treatments on the fluoride removal from water by three mineral structures and their characterization. *Journal of Fluorine Chemistry, 213*, 42–50. https://doi.org/10.1016/j.jfluchem.2018.07.002.

Crisafully, R., Milhome, M. A. L., Cavalcante, R. M., Silveira, E. R., De Keukeleire, D., & Nascimento, R. F. (2008). Removal of some polycyclic aromatic hydrocarbons from petrochemical wastewater using low-cost adsorbents of natural origin. *Bioresource Technology*. https://doi.org/10.1016/j.biortech.2007.08.041.

Dávila-Estrada, M., Ramírez-García, J. J., Díaz-Nava, M. C., & Solache-Ríos, M. (2016). Sorption of 17α-ethinylestradiol by surfactant-modified zeolite-rich tuff from aqueous solutions. *Water, Air, and Soil Pollution*. https://doi.org/10.1007/s11270-016-2850-y.

de Gennaro, B., Catalanotti, L., Bowman, R. S., & Mercurio, M. (2014). Anion exchange selectivity of surfactant modified clinoptilolite-rich tuff for environmental remediation. *Journal of Colloid and Interface Science*. https://doi.org/10.1016/j.jcis.2014.05.037.

Ghauch, A., Tuqan, A., & Assi, H. A. (2009). Antibiotic removal from water: Elimination of amoxicillin and ampicillin by microscale and nanoscale iron particles. *Environmental Pollution, 157*(5), 1626–1635. https://doi.org/10.1016/j.envpol.2008.12.024.

Ghimire, S., Flury, M., Scheenstra, E. J., & Miles, C. A. (2019). Jo ur na l P re of. *Science of the Total Environment, 135577*. https://doi.org/10.1016/j.scitotenv.2019.135577.

Grenni, P., Ancona, V., & Barra Caracciolo, A. (2018). Ecological effects of antibiotics on natural ecosystems: A review. *Microchemical Journal, 136*, 25–39. https://doi.org/10.1016/j.microc.2017.02.006.

Guan, H., Bestland, E., Zhu, C., Zhu, H., Albertsdottir, D., Hutson, J., et al. (2010). Variation in performance of surfactant loading and resulting nitrate removal among four selected natural zeolites. *Journal of Hazardous Materials*. https://doi.org/10.1016/j.jhazmat.2010.07.069.

Hansch, C., Leo, A., & Hoek-man, D. (1996). Book Reviews. *Journal of Medicinal Chemistry, 39*, 1189–1190.

Hashemian, S., Ardakani, M. K., & Salehifar, H. (2013). Kinetics and thermodynamics of adsorption methylene blue onto tea waste/CuFe2O4 composite. *American Journal of Analytical Chemistry, 04*(07), 1–7. https://doi.org/10.4236/ajac.2013.47A001.

Hirsch, R., Ternes, T., Haberer, K., & Kratz, K. L. (1999). Occurrence of antibiotics in the aquatic environment. *Science of the Total Environment, 225*(1–2), 109–118. https://doi.org/10.1016/S0048-9697(98)00337-4.

Ho, Y. S., & McKay, G. (1999). Pseudo-second order model for sorption processes. *Process Biochemistry, 34*(5), 451–465. https://doi.org/10.1016/S0032-9592(98)00112-5.

Kemper, N. (2008). Veterinary antibiotics in the aquatic and terrestrial environment. *Ecological Indicators, 8*(1), 1–13. https://doi.org/10.1016/j.ecolind.2007.06.002.

Khan, S. J., & Ongerth, J. E. (2004). Modelling of pharmaceutical residues in Australian sewage by quantities of use and fugacity calculations. *Chemosphere, 54*(3), 355–367. https://doi.org/10.1016/j.chemosphere.2003.07.001.

Khan, M. N., & Sarwar, A. (2007). Determination of points of zero charge of natural and treated adsorbents. *Surface Review and Letters, 14*(3), 461–469. https://doi.org/10.1142/S0218625X07009517.

Klein, E. Y., Van Boeckel, T. P., Martinez, E. M., Pant, S., Gandra, S., Levin, S. A., et al. (2018). Global increase and geographic convergence in antibiotic consumption between 2000 and 2015. *Proceedings of the National Academy of Sciences*, 201717295. https://doi.org/10.1073/pnas.1717295115

Kong, X., Han, Z., Zhang, W., Song, L., & Li, H. (2016). Synthesis of zeolite-supported microscale zero-valent iron for the removal of Cr6+and Cd2+from aqueous solution. *Journal of Environmental Management, 169*, 84–90. https://doi.org/10.1016/j.jenvman.2015.12.022.

Krajišnik, D., Daković, A., Milojević, M., Malenović, A., Kragović, M., Bogdanović, D. B., et al. (2011). Properties of diclofenac sodium sorption onto natural zeolite modified with cetylpyridinium chloride. *Colloids and Surfaces B: Biointerfaces, 83*(1), 165–172. https://doi.org/10.1016/j.colsurfb.2010.11.024.

Kümmerer, K. (2009). Antibiotics in the aquatic environment - A review - Part II. *Chemosphere*. https://doi.org/10.1016/j.chemosphere.2008.12.006

Langmuir, I. (1917). The constitution and fundamental properties of solids and liquids. II. Liquids. *Journal of the American Chemical Society, 39*(9), 1848–1906. https://doi.org/10.1021/ja02254a006.

Li, W. C. (2014). Occurrence, sources, and fate of pharmaceuticals in aquatic environment and soil. *Environmental Pollution, 187*, 193–201. https://doi.org/10.1016/j.envpol.2014.01.015.

Li, Z., Yuansheng, D., & Hanlie, H. (2008). Transport of micelles of cationic surfactants through clinoptilolite zeolite. *Microporous and Mesoporous Materials*. https://doi.org/10.1016/j.micromeso.2008.05.006.

Low, M. J. D. (1960). Kinetics of chemisorption of gases on solids. *Chemical Reviews, 60*(3), 267–312. https://doi.org/10.1021/cr60205a003.

Mirzaei, R., Yunesian, M., Nasseri, S., Gholami, M., Jalilzadeh, E., Shoeibi, S., & Mesdaghinia, A. (2018). Occurrence and fate of most prescribed antibiotics in different water environments of Tehran, Iran. *Science of the Total Environment, 619–620*, 446–459. https://doi.org/10.1016/j.scitotenv.2017.07.272.

Misaelides, P. (2011). Application of natural zeolites in environmental remediation: A short review. *Microporous and Mesoporous Materials*. https://doi.org/10.1016/j.micromeso.2011.03.024.

Montes-Luna, A. D. J., Fuentes-López, N. C., Perera-Mercado, Y. A., Pérez-Camacho, O., Castruita-de León, G., García-Rodríguez, S. P., & García-Zamora, M. (2015). Caracterización de clinoptilolita natural y modificada con Ca2+por distintos métodos físico-químicos para su posible aplicación en procesos de separación de gases. *Superficies y Vacio*.

Mozgawa, W., Król, M., & Bajda, T. (2011). IR spectra in the studies of anion sorption on natural sorbents. In *Journal of Molecular Structure*. https://doi.org/10.1016/j.molstruc.2010.11.070

Pang, G.-F. (2018). *β-Lactams. Analytical methods for food safety by mass spectrometry*. https://doi.org/10.1016/B978-0-12-814165-6.00005-1

Rakić, V., Rajić, N., Daković, A., & Auroux, A. (2013). The adsorption of salicylic acid, acetylsalicylic acid and atenolol from aqueous solutions onto natural zeolites and clays: Clinoptilolite, bentonite and kaolin. *Microporous and Mesoporous Materials, 166*, 185–194. https://doi.org/10.1016/j.micromeso.2012.04.049.

Rasouli, M., Yaghobi, N., Chitsazan, S., & Sayyar, M. H. (2012). Influence of monovalent cations ion-exchange on zeolite ZSM-5 in separation of para-xylene from xylene mixture. *Microporous and Mesoporous Materials*. https://doi.org/10.1016/j.micromeso.2011.09.013.

Reeve, P. J., & Fallowfield, H. J. (2018). Natural and surfactant modified zeolites: A review of their applications for water remediation with a focus on surfactant desorption and toxicity towards microorganisms. *Journal of Environmental Management., 205*, 253–261. https://doi.org/10.1016/j.jenvman.2017.09.077.

Rivera-Gutiérrez, E., Ramírez-García, J. J., Pavón Romero, S. H., Rodríguez, M. M., Ramírez-Serrano, A., & Jiménez-Marin, A. (2020). Dicloxacillin degradation with free-living bacteria. *Water, Air, and Soil Pollution, 231*(2), 1–13. https://doi.org/10.1007/s11270-020-4456-7.

Rodriguez-Narvaez, O. M., Peralta-Hernandez, J. M., Goonetilleke, A., & Bandala, E. R. (2017). Treatment technologies for emerging contaminants in water: A review. *Chemical Engineering Journal, 323*, 361–380. https://doi.org/10.1016/j.cej.2017.04.106.

Roxana Elena Apreutesei, C. C., & Carmen Teodosiu. (2008). Surfactant-modified natural zeolites for environmental applications in water purification. *Environmental Engineering and Management Journal, 7*(2), 149–161.

Rožić, M., & Miljanić, S. (2011). Sorption of HDTMA cations on Croatian natural mordenite tuff. *Journal of Hazardous Materials*. https://doi.org/10.1016/j.jhazmat.2010.09.050.

Salgado-Gómez, N., Macedo-Miranda, M. G., & Olguín, M. T. (2014). Chromium VI adsorption from sodium chromate and potassium dichromate aqueous systems by hexadecyltrimethylammonium-modified zeolite-rich tuff. *Applied Clay Science, 95*, 197–204. https://doi.org/10.1016/j.clay.2014.04.013.

Sprynskyy, M., Golembiewski, R., Trykowski, G., & Buszewski, B. (2010). Heterogeneity and hierarchy of clinoptilolite porosity. *Journal of Physics and Chemistry of Solids*. https://doi.org/10.1016/j.jpcs.2010.05.006.

Torres-Pérez, J., Solache-Ríos, M., & Olguín, M. T. (2007). Sorption of azo dyes onto a Mexican surfactant-modified clinoptilolite-rich tuff. *Separation Science and Technology, 42*(2), 299–318. https://doi.org/10.1080/01496390601069879.

Turiel, E., Perez-Conde, C., & Martin-Esteban, A. (2003). Assessment of the cross-reactivity and binding sites characterisation of a propazine-imprinted polymer using the Langmuir-Freundlich isotherm. *Analyst, 128*(2), 137–141. https://doi.org/10.1039/b210712k.

Vasquez, M. I., Lambrianides, A., Schneider, M., Kümmerer, K., & Fatta-Kassinos, D. (2014). Environmental side effects of pharmaceutical cocktails: What we know and what we should know. *Journal of Hazardous Materials, 279*, 169–189. https://doi.org/10.1016/j.jhazmat.2014.06.069.

Villegas-Guzman, P., Silva-Agredo, J., Giraldo-Aguirre, A. L., Flórez-Acosta, O., Petrier, C., & Torres-Palma, R. A. (2015). Enhancement and inhibition effects of water matrices during the sonochemical degradation of the antibiotic dicloxacillin. *Ultrasonics Sonochemistry, 22*, 211–219. https://doi.org/10.1016/j.ultsonch.2014.07.006.

Weng, X., Cai, W., Lan, R., Sun, Q., & Chen, Z. (2018). Simultaneous removal of amoxicillin, ampicillin and penicillin by clay supported Fe/Ni bimetallic nanoparticles. *Environmental Pollution, 236*, 562–569. https://doi.org/10.1016/j.envpol.2018.01.100.

Wu, C., Spongberg, A. L., & Witter, J. D. (2009). Sorption and biodegradation of selected antibiotics in biosolids. *Journal of Environmental Science and Health - Part A Toxic/Hazardous Substances and Environmental Engineering, 44*(5), 454–461. https://doi.org/10.1080/10934520902719779.